Science and Engineering of Composite Materials 13, 65-77 (2006)

Static and Dynamic Wetability of Molten Al on Al_2O_3 and ZrO_2 Substrates

Craig Townsend [1], Hani Henein [1], Steve Corbin [2], Prasad Apte [3]

[1]*Advanced Materials and Processing Lab, University of Alberta, Edmonton, Alberta*
[2]*University of Waterloo, Waterloo, Ontario*
[3]*Praxair formerly with Westaim Corp., Fort Saskatchewan, Alberta*
Canada

ABSTRACT

In the fabrication of aluminum MMCs, the interface between metal and ceramic reinforcement may be associated with an oxide layer which plays a key role in the structure and properties of the MMC. This paper outlines some understanding into the breakdown of this oxide layer in aluminum and the corresponding contact between metal and reinforcement. The system under review consists of Al metal with 0 or 10%Mg alloy addition and ZrO_2 and Al_2O_3 ceramic substrate material. It is shown that three conditions are required to destabilize the surface oxide on the aluminum: high temperature, alloying the melt and an atmosphere of nitrogen. This allows the melt to flow freely over the substrate resulting in regions of extensive reaction between melt and substrate and the formation of Al_3Zr as one of the reaction products. It is also shown that impact of droplets on a ceramic substrate is not sufficient to break down the oxide layer on the droplets. These results highlight the need to develop controlled processing methodologies for the fabrication of MMCs with desired properties.

INTRODUCTION

Thin film aluminum-oxide ceramic-based composites are useful in applications where strength to weight ratios are important in rigid components but metallic surface properties are desired. Metal-matrix composites are of great interest in the aerospace, automotive and energy industries for improved wear resistance applications and high temperature environments /1/. Although the processing routes and final products are different, the main obstacle in manufacturing both these types of composites today is the formation of a good bond between the metal and ceramic /2,3/. A secondary obstacle seen in some cases are unwanted reactions that occur at the interface between the metal and reinforcement /2,4/. Understanding the phenomena occurring at the interface of the metal and the ceramic during the processing of the MMC is critical to the successful processing and application of these materials. This is particularly critical for aluminum alloys as aluminum has a very high propensity to form an oxide coating on its free surface. This oxide will play an important role in the type, nature and properties of the interface between metal and reinforcement.

A series of experiments were carried out to develop such a fundamental understanding for the $Al:Al_2O_3$ and $Al:ZrO_2$ composites systems during processing. The experimental variables included temperature of contact, 973 to 1273 K, gas atmosphere, Ar and N_2, Mg as an alloying element in the aluminum matrix and a means to impact the droplets onto the substrate. Two types of experiments were therefore carried out: static and dynamic. For the static experiments, the metal and substrate were placed in contact at a desired temperature for a finite period of time. In dynamic experiments, a spray of metal droplets was generated and deposited onto the ceramic substrate. Subsequently, the interface was studied using SEM. The mechanisms associated

with the metal-substrate bonding were explored with the aid of FACT /5/.

EXPERIMENTAL CONDITIONS

Materials

All of the ceramic substrates were tape cast then fired at the Westaim Labs. Density measurements using Archimedes principle showed that the Al_2O_3 was approximately 94% dense while the ZrO_2 was fully dense. Under SEM examination, the substrate materials showed slight porosity at the surface of the ZrO_2 and throughout the cross section of Al_2O_3. With 94% of full densification the pores in the Al_2O_3 were not interconnected. The substrates used for the static tests measured 0.025x0.025x0.001 m; while the dimensions of substrates for the spray tests were 0.025 m diameter and 0.001 m thick.

Commercial purity aluminum was used for some of the static tests. It contained about 98.4% Al and 1.14 % Fe and 0.43% Si. The aluminum used for the dynamic tests was 99.9%Al granules. For the Al-Mg alloy used in both static and dynamic tests, industrial purity Mg was mixed with the 99.9% Al granules to prepare a Al-Mg alloy having 10% Mg.

Apparatus

The samples for static tests were placed in graphite boats for the duration of the experiment in a layered ZrO_2-metal-Al_2O_3 configuration as shown in Figure 1. The boat was preheated in the furnace for approximately 15 minutes, then placed into the hot zone of the furnace for 3 hours. In the preheat and hot zones of the furnace, the atmosphere was controlled by supplying a constant flow of the test gas, Ar or N_2. Samples were cooled in the furnace then subsequently removed for visual inspection, metallographic preparation and SEM examination.

The spray or dynamic tests were conducted in an impulse atomizer, which atomized the melt. Melt droplets then deposited onto the heated ceramic substrate. The contact between the molten spray and the heated substrate is shown schematically in Figure 2. The ceramic substrate was heated to a desired temperature using a substrate heater. The whole apparatus is contained in an airtight cylinder where the composition of the atmosphere can be controlled. The Impulse Atomization has been described elsewhere /6,7/. However, it is important to point out that the ability of this technique to generate droplets in a narrow size distribution provided us with the desired control on the droplet temperature and size on contact with the substrates.

For the spray test, a number of 50 mm diameter graphite boats were used to contain the substrate material and the deposited liquid metal. The boats were loaded onto 1 of 2 trays and manually manipulated using a metal arm which extended through the tower wall. The substrate heater was mounted between the trays with a type C thermocouple on a pivot mounted to read the temperature of the outside of the graphite boat.

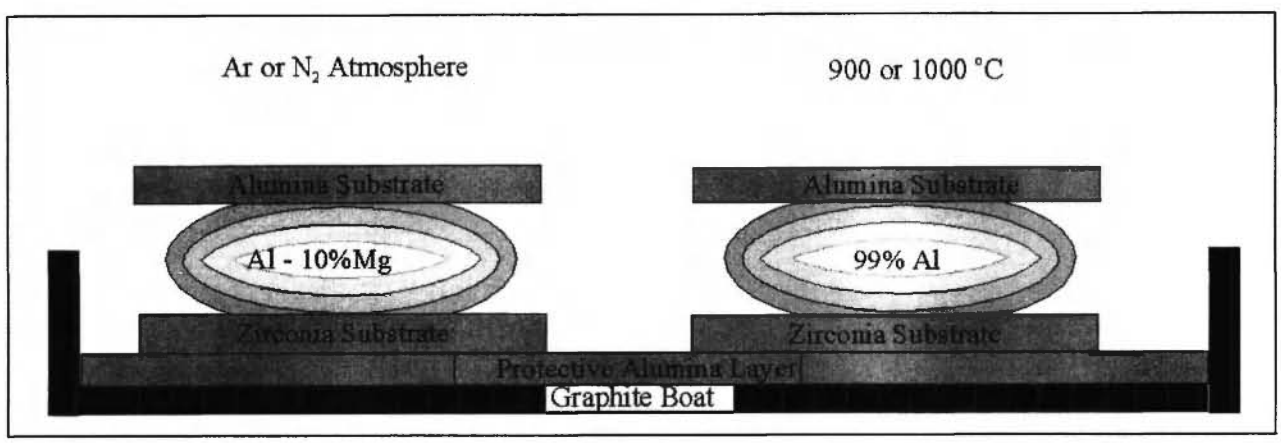

Fig. 1: Static test configuration showing metal and ceramic contact before being placed in the furnace.

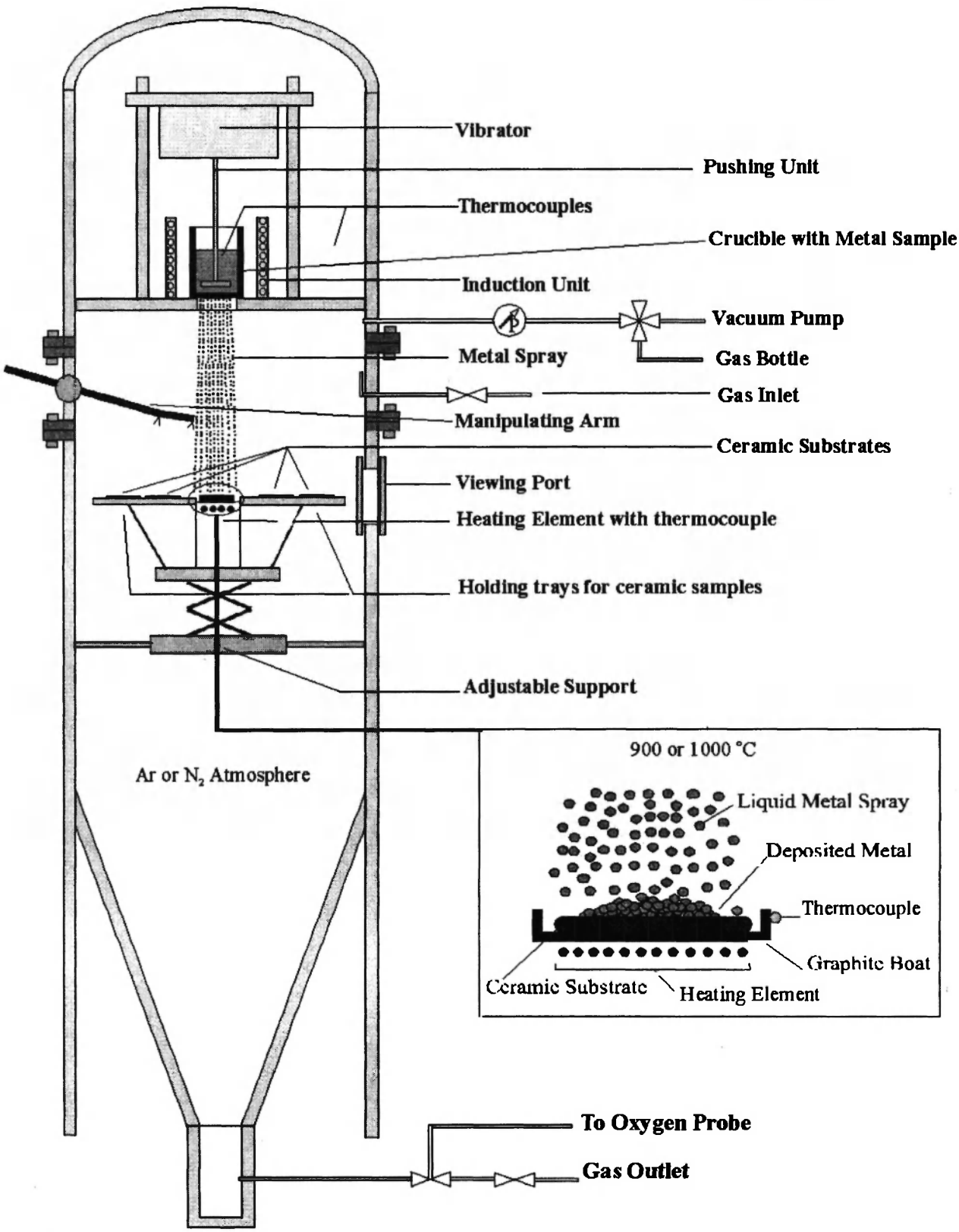

Fig. 2: Schematic of spray deposition illustrating atomized melt sprayed onto porous heated ceramic substrate.

A second type C thermocouple was placed in the melt crucible.

A typical spray deposition experiment proceeded as follows. The tower was evacuated and purged with the desired gas atmosphere, Ar or N_2, three times. The Ar or N_2 were then purged through the tower until the oxygen reading on the Centaur oxygen analyzer was less than 100 ppm. Throughout the remainder of the experiment a small purge of Ar or N_2 was continued and the pressure in the tower was maintained at slightly above atmospheric pressure to minimize oxygen infiltration into the tower. The metal in the crucible was then melted and maintained at the desired temperature. Subsequently, the substrate heater was started and the substrate was maintained at a constant temperature for 15 min prior to commencing atomization. Contact time between metal and substrate was measured from the time the first drops of liquid metal reached the substrate surface to the time when the graphite boat was moved to the cooling tray. The samples were allowed to cool to room temperature prior to exposing them to atmospheric conditions for visual examination, metallographic preparation and SEM analysis.

Test Conditions

The test conditions used for the static and spray tests are listed in Table I. All test conditions shown below were carried out using both Ar and N_2 atmospheres and with both ZrO_2 and Al_2O_3 substrates. A total of 16 static samples and 16 spray samples were tested. It should be added that except for the static tests with N_2, all other runs were carried out using industrial grade bottled gases. Standard plant N_2 was used for the static tests.

The following atomizing conditions were used for the spray tests. Graphite nozzle plates having 37 orifices of 0.4 mm diameter were prepared. The nozzle plates were fitted in graphite crucibles and the melting was carried out using an induction furnace.

Samples were cut normal to the metal-ceramic interface using a high-speed diamond cutting wheel. They were then polished, the final polish being with a suspension containing 0.05-micron alumina. Samples were then carbon coated and placed in a Hitachi S2700 SEM with an attached Link eXL EDX analysis system. The SEM has a turreted windowless detector for light element detection.

Table I
Test conditions

Metal	Substrate Temperature (°C)	Melt Temperature (°C)	Contact Time
	Static Tests		
Al	900	900	3 hrs
Al-10%Mg	900	900	3 hrs
Al	1000	1000	3 hrs
Al-10%Mg	1000	1000	3hrs
	Spray Tests		
Al	680	700, 850, 1000	1 min
Al-10%Mg	680	820	5 min

RESULTS

As the samples were removed from the respective furnaces in static and dynamic tests, the nature of contact between metal and ceramic was observed and the strength of the bond of the interface was noted through subsequent sample handling and analysis. The interface between the metal and ceramic substrate was observed using the SEM, and the nature of reaction products (when detected) was analyzed. These observations and results are presented and discussed below.

Visual Inspection of Samples

In the static tests, the metal clearly retained its shape sandwiched between the Al_2O_3 and the ZrO_2 substrates. There was some bulging of the metal sample at its sides as shown schematically in Figure 1. This is clearly due to the fact that the metal was molten and that the oxide coating the metal was of sufficient strength to contain

the melt. This oxide layer on the metal occurred from the exposure of the metal to the atmosphere prior to carrying out these experiments. In one case, the Al-10Mg tested under N_2 and at 1000 °C, the metal flowed readily and coated the substrate materials. It even flowed below the ZrO_2 substrate and wetted the graphite boat supporting the samples. Metal thickness as little as 10 μm was observed on the underside of the ZrO_2 substrate. This sample will be further discussed below.

In the spray tests, the droplets appeared to retain their geometrical integrity and did not flow and coalesce on the substrate (see Figure 3). This is in part due to the fact that the period of atomization was kept short. But it is equally clear from this that the momentum of the droplets was not sufficient to break the oxide coating that formed on the droplet surface. Note that even though the starting oxygen content in the tower was low (< 100 ppm), the high reactivity of aluminum would result in oxidation of the surface of the droplets upon atomization. From previous work /8/, we can estimate the droplet d50 of 756 microns and the initial droplet velocity exiting the orifice to be 2.17 m/s, respectively. With the substrate located 0.34 m below the nozzle, would yield an estimated droplet momentum on impact with the substrate of 1.33×10^{-6} kg.m/s and an impact force of 3.75×10^{-10} N.

All static and dynamic test samples showed strong bonding between the metal and substrate. The bond was retained through the period when the metal on the substrates solidified and cooled to room temperature. In addition, no debonding occurred with any samples during metallographic sample preparation for SEM examination. (i.e. sample cutting with the high speed saw).

SEM Analysis

Cross sectional analysis of the sample interfaces using the SEM was carried out on both static and dynamic samples. With one exception, the results revealed a linear interface between metal and ceramic with little or no reaction products at the interface. Figures 4 and 5 are for Al_2O_3 and ZrO_2 substrates respectively and are representative of the interfaces seen. No reaction products were detected at or near the interface at up to magnifications of 6000 X.

The one exception noted above was for the following experimental conditions. The sample was

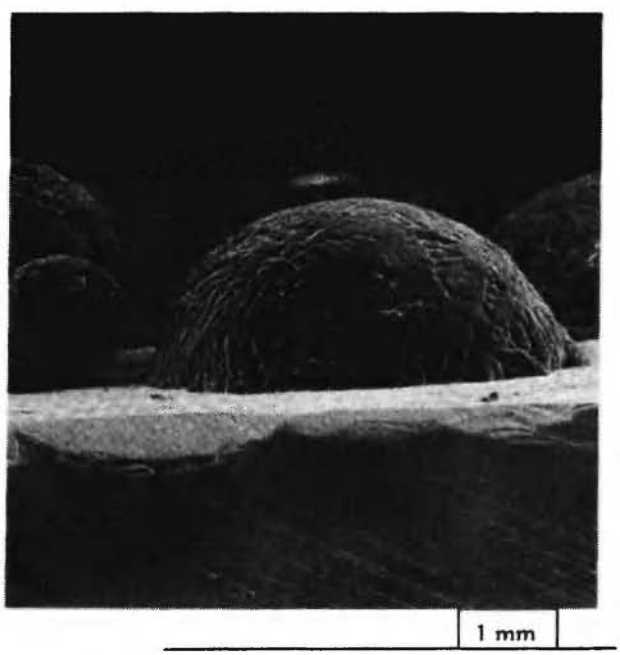

Fig. 3: SEM of the ZrO_2 substrate surface snowing some sparse deposition of Al-Mg spray droplets.

Fig. 4: SEM Image of the Al-Mg/Al_2O_3 interface for a static test at 900 °C, 3 hrs contact time in a Nitrogen atmosphere.

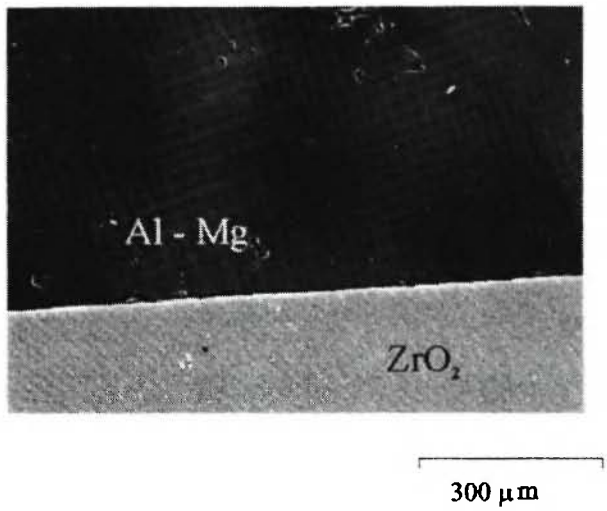

Fig. 5: SEM Image of the Al-Mg/ZrO_2 interface for a static test at 1000 °C, 3 hrs contact time and a Nitrogen atmosphere.

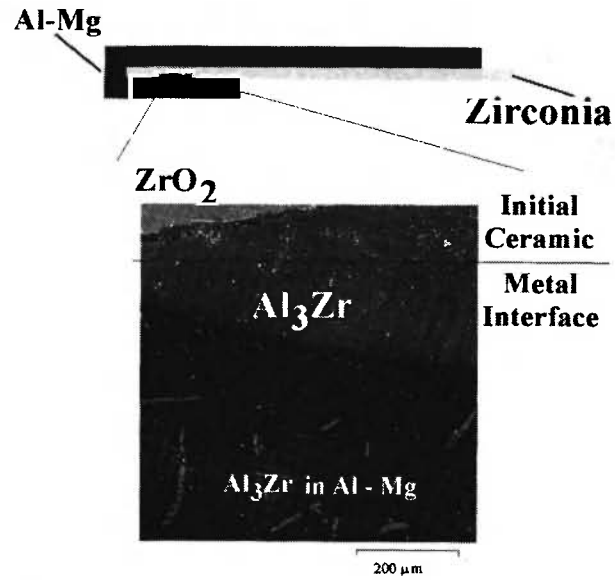

Fig. 6a: SEM Image of the Al-Mg/ZrO_2 interface for a static test at 1000 °C, 3hrs contact time in a Nitrogen atmosphere. Note that the SEM image is of the underside of the zirconia in the schematic given above. The Al-Mg alloy has spread to cover the underside of the zirconia which is the surface between the zirconia and the protective alumina layer shown in Figure 1.

from a static test carried out in a N_2 atmosphere, at 1000 °C and 3 hrs contact time between the Al-10Mg alloy and the Al_2O_3 and ZrO_2 ceramic substrates. Figure 6 shows an X-Ray elemental dot map of the reacted region. Extensive reaction products are evident with ZrO_2 on its underside.

Clearly, there is a heavy concentration of Zr and Al at the interface between metal and ceramic as well as concentrated regions of Zr and Al in the metal. We suggest that this is a reaction product, namely Al_3Zr. In addition, Mg, Al and O were detected with a stoichiometry close to that of $MgAl_2O_4$. This region is just below the massive region of Al and Zr concentration. In the regions where the alloy had been originally placed on top of the ZrO_2 substrate, no reaction products were detected. The interface appeared to be similar to that shown in Figure 5. Note that Hass /9/ reported that after exposure to air the thickness of the alumina on aluminum metal could be as thick as 4.5 to 9 nanometers at room temperature for 6 days to two months. It is evident that even such a thin oxide layer can effectively impede the interfacial reaction. At the metal-Al_2O_3 interface, some $MgAl_2O_4$ spinel was found in areas where the metal had spread. Again no reaction was observed where the metal was originally in contact with the Al_2O_3 substrate.

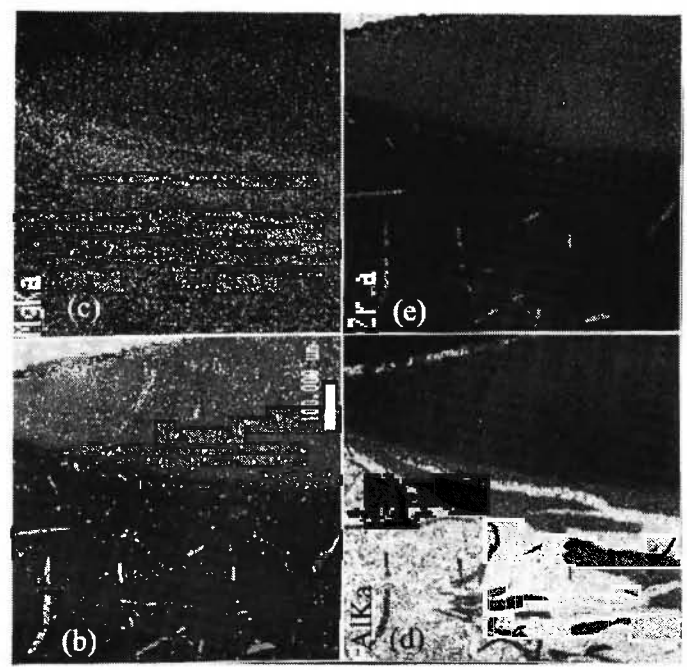

Fig. 6b to 6e: SEM X-Ray Dot Map of the Al-Mg/ZrO_2 interface showing reaction products. b) SEM image, c) Mg map, d) Al map, e) Zr map.

DISCUSSION

From the observations presented earlier, it appears that aluminum bonds best to the ceramic substrates when the experimental conditions include a combination of high temperature, 1000 °C, a nitrogen atmosphere, an Al-Mg alloy and time. Recall that observations of the deposited droplets in dynamic tests did not reveal any flow of the alloy. All droplets kept a hemispherical shape as shown in Figure 3, while for the case of static tests with the ZrO_2 substrate the alloy flowed readily and reacted on the underside of the ZrO_2 substrate. We will attempt to explain these observations using published data and a thermodynamic analysis of the system. Thus, a fundamental understanding of the conditions required for contact between aluminum and ceramic can be gained.

Effect of Temperature

It has been shown that the surface oxide layer on molten Al could be evaporated at temperatures above about 1000 °C. This was reported from tests using sessile drop experiments to measure the interfacial tension of aluminum /4/. Earlier, an analysis of the surface properties of aluminum by Kaptay discussed the role of alumina on the surface properties of molten aluminum /9/. He clearly showed that the surface tension of molten aluminum covered with alumina decreased with increasing temperature. In addition, the surface tension of molten alumina increased with decreasing temperature. The surface tension of aluminum covered with alumina seemed to coincide with the surface tension of molten alumina at the melting point of alumina. This suggests that at temperatures lower than the melting point of alumina, the surface tension of aluminum is influenced by that of alumina. Furthermore, it was suggested that the increased thermodynamic stability of Al_2O gas with increasing temperature contributes to the reduced surface tension of aluminum.

Clearly, elevated temperatures will contribute to a weakened oxide coating on the metal. In addition, it is evident that the oxide coating on the metal plays a dominant role in the behavior and characteristics of molten aluminum and its alloys. In order to enhance wetting between the molten metal and a substrate or reinforcement (in MMC processing), the surface oxide layer must be weakened. This may be achieved by increasing the melt temperature. However, in the light of our experiments, elevated temperature alone did not result in extensive wetting between metal and substrate nor the extensive reaction observed between the aluminum alloy and the ZrO_2 substrate. Recall that static samples tested with Al in an Ar atmosphere and at 1000°C did not result in any interfacial reactions even after 3 hours of contact time.

Effect of Magnesium

It is well established in the literature that magnesium is surface active in aluminum alloys and that it reduces the surface tension of aluminum /10-12/. This behavior of magnesium was clearly observed in this work with the sample which exhibited metal spreading, see Figures 7a and 7b. Similar behavior was also observed in the other samples, which did not exhibit metal flow. A point scan of Mg near the metal-alumina interface is shown in Figure 7c. A similar scan at the alloy-zirconia interface is shown in Figure 8. It is clear that the concentration of Mg near the alloy surface is higher than it is adjacent to the metal surface. A similar scan was carried out on a sample exposed to an Argon atmosphere. It also exhibited considerable segregation of Mg to the surface of the metal.

Once the solute Mg in the liquid alloy reaches the surface, there is a driving force for the Mg to vaporize. The actions of Mg in the alloy at the surface of the liquid metal (Mg) can be described by the following equations:

$$\underline{Mg} = Mg_{(g)} \quad (1)$$

$$\Delta G^{o} = -RT \ln (P_{Mg}/a_{Mg}) \quad (2)$$

where ΔG^{o} is the standard Gibbs Molar Free Energy of magnesium when dissolved in the aluminum and is in equilibrium with magnesium vapour, R is the universal gas constant, T is the temperature, P_{Mg} is the vapour pressure of magnesium above the melt and a_{Mg} is the activity of magnesium in the molten aluminum.

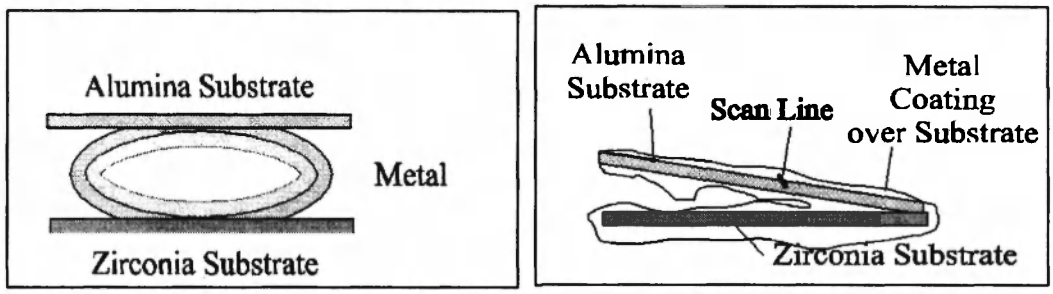

(a) (b)

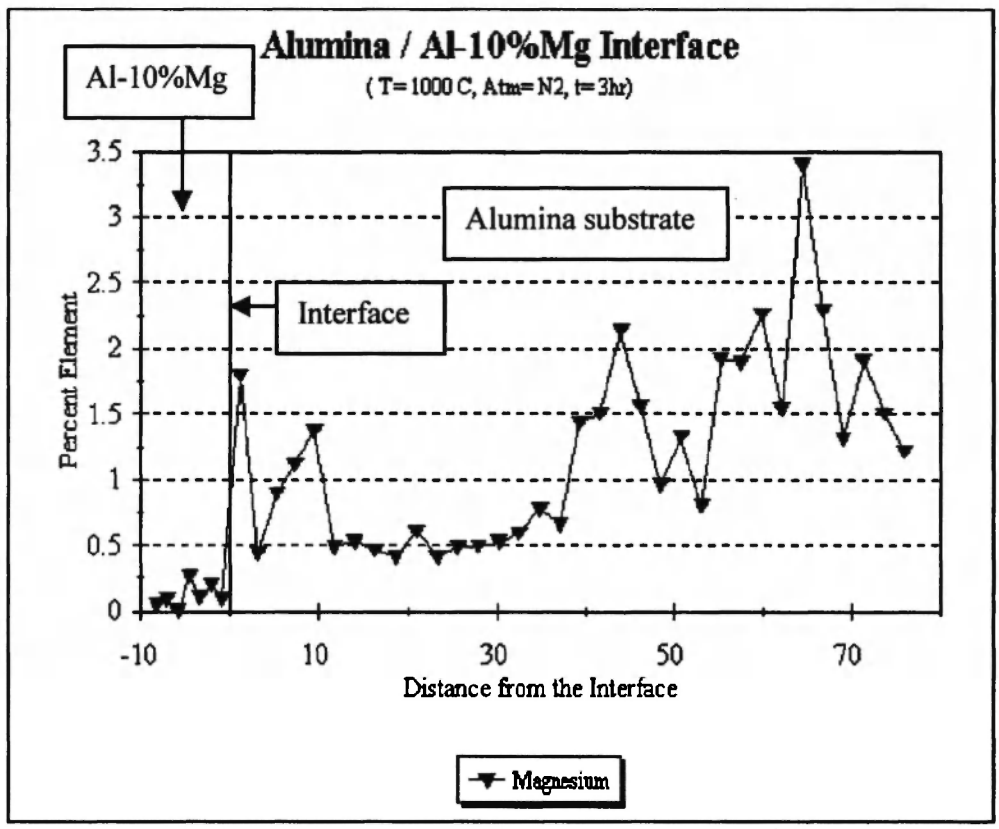

(c)

Fig. 7: Alumina-Al-10%Mg interface at 1000 °C in nitrogen atmosphere with 3 hours contact time in a static test (a) original confirmation, (b) configuration after spontaneous wetting, (c) Plot of Mg values from the X-Ray Point Scan taken across the interface.

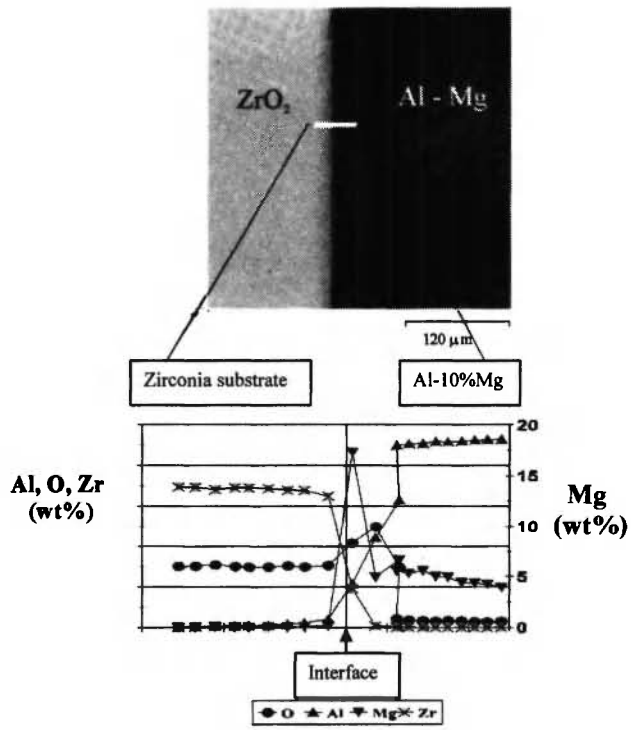

Fig. 8: Line scan across Al-Mg/ZrO_2 interface for static sample at 1000 °C, in nitrogen for 3 hours.

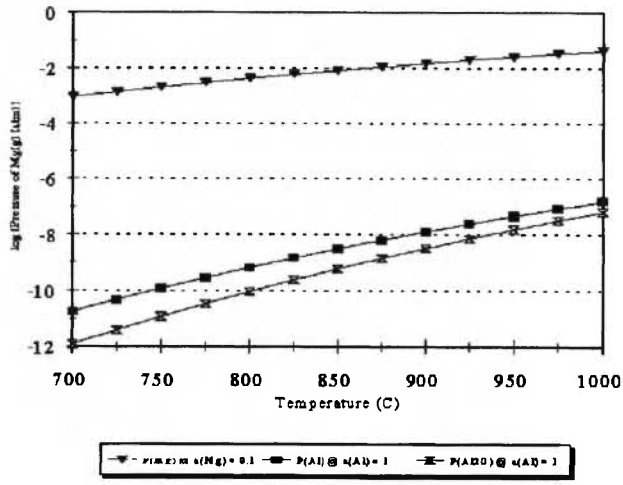

Fig. 9: FACT[5] generated equilibrium pressures for Mg (a[Mg] = 0.1), Al (a[Al] = 1) and Al_2O (at the equilibrium Al pressure and 10 ppm O_2).

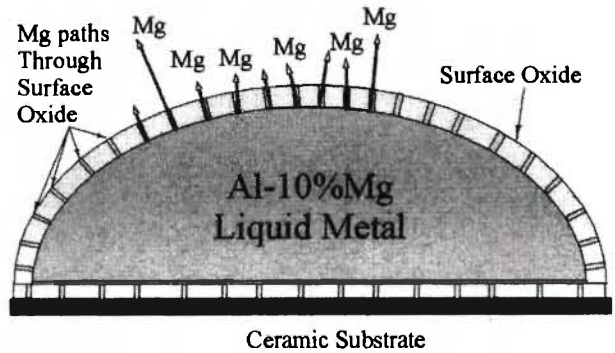

Fig. 10: Schematic of Mg segregating to the melt surface, diffusing through the surface oxide disrupting the surface.

The Bulletin of Alloy Phase Diagrams considers the liquid phase being close to ideal with a slight negative deviation.[13] The current calculations considered the alloy as ideal. As such, Figure 9 shows the equilibrium vapor pressure of Mg above a 10%Mg alloy in comparison with the equilibrium pressures of Al vapor and Al_2O gas above pure Al. Given that the Mg added to the melt is surface active as described above, the high vapor pressure will build up under the surface oxide covering the liquid metal. Should the surface oxide be weakened due to high temperature as previously established and Mg vapour pressure build up underneath the oxide. Thus, the presence of magnesium build up at the metal surface or at the metal-oxide coating interface will result in the formation of spinel as well as the breakdown of surface oxide layer shown schematically in Figure 10. It is known that when Mg(g) reduces ZrO_2, the latter turns black.[14] All ZrO_2 samples in static and dynamic trials tested with the Al-Mg alloy turned black. Therefore, Mg(g) did escape into the atmosphere.

The presence of such relatively large amount of Mg near the surface would also affect the chemical and physical nature of the surface oxide. An SEM photograph of the alloy surface of the sample exposed to 1000 °C in Ar is shown in Figures 11a and 11b. The remains of the original room temperature surface oxide are visible as 'fractured' platelets on the surface of the alloy. X-ray analysis of these platelets reveals that the composition closely resembles that of the spinel $MgAl_2O_4$. X-Ray analysis of the remaining surface appearing as rough granules seems to be richer in oxygen than the platelets. This indicates that Mg alloyed

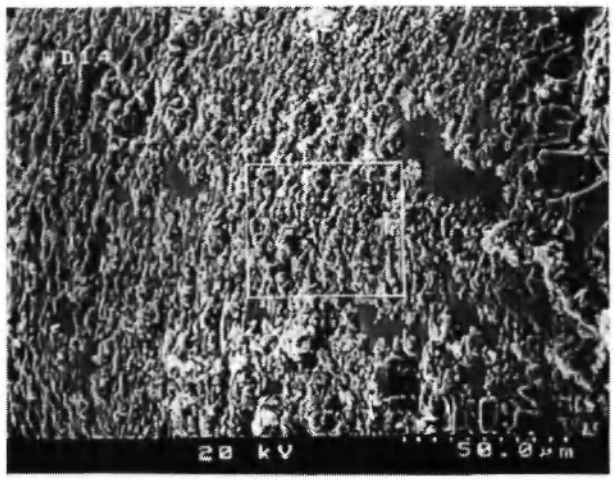

(a)

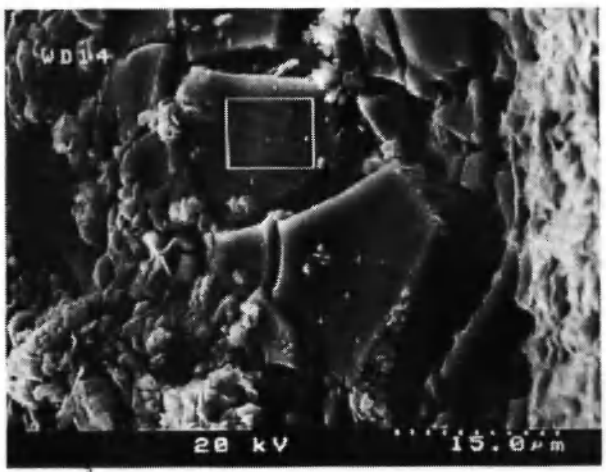

(b)

Fig. 11: SEM image of the Al-Mg surface showing the ruptured surface oxide of spinel composition. The sample was exposed to an Ar atmosphere for 3hrs at 1000 °C.

with aluminum does cause a rupture of the surface oxide at high temperatures and modifies the surface chemistry of the surface oxide, which subsequently forms. Note that the spinel melts at a lower temperature than alumina. This will add to the destabilization of the surface oxide at elevated temperatures. However, the surface oxide appears to still have sufficient strength to stop the liquid metal from spreading. Clearly, temperature and Mg alloying together are still not sufficient to destabilize the oxide coating covering the alloy. This is evident from the fact that Al-Mg alloys tested at 1000 C in Ar did not spread out but was contained by the surface oxide covering the alloy.

Effect of Nitrogen Atmosphere

The Lanxide Corporation has patented an MMC fabrication technique, which acknowledges the need for using N_2 in order for liquid Al-Mg to wet alumina and zirconia at elevated temperatures. Figure 12 is of the sample which was made under the same conditions as Figure 11 with the exception that N_2 was the gas atmosphere instead of Ar. The surface formations on the sample in Figure 12 are much greater in numbers, size and variety than those in Figure 11 indicating a more destabilized surface oxide layer in N_2 than in Ar. In order to understand this, we need to examine the equilibrium between aluminum and nitrogen.

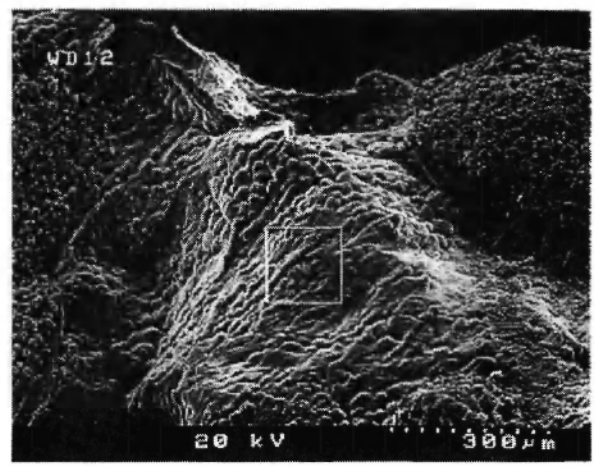

Fig. 12: SEM image of the Al-Mg surface showing the ruptured and rough metal surface of spinel composition. Test conditions were 1000 C and 3hr of exposure time to a Nitrogen Atmosphere .

Consider Al(g) is in equilibrium with molten aluminum. The reaction between Al(g) and N_2 is given by equation (3):

$$Al_{(g)} + 0.5\ N_2 = AlN_{(s)} \quad (3)$$

The equilibrium N_2 pressure for Equation (3) is calculated as a function of temperature and is shown in Figure 13. Clearly, with N_2 present in the furnace at 1 atm pressure, there is a significant driving force for AlN to form. Recall that N_2 was continuously supplied to the furnaces in both static and dynamic experiments and the total pressure in the atmosphere was maintained at 1 atm. Clearly, this regular supply of N_2 will continue to provide a constant driving force for the formation of AlN and the continued evaporation of Al(g) from the molten metal. Unfortunately, we were not able to detect significant amounts of AlN in any of our samples. This was in part beyond the capabilities of our SEM. The low magnitude of the Al(g) equilibrium vapor pressure (see Figure 9) may also indicate that AlN may only be present in trace amounts. As with the effect of temperature and magnesium, N_2 alone was not sufficient to break the oxide layer and cause spreading of the molten metal over the ceramic substrate.

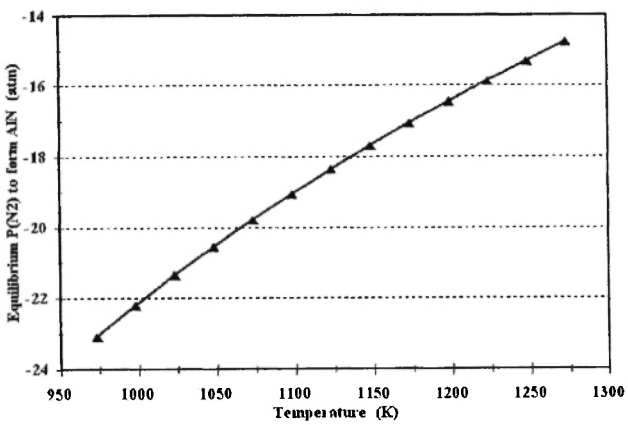

Fig. 13: Equilibrium partial pressure of nitrogen in equilibrium with Al vapor for the formation of AlN.

Reaction Mechanism

In an attempt to explain the presence of the extensive reaction products observed in Figure 6, a Thermodynamic Stability Diagram was calculated for the Al-Mg-Zr-O_2-N_2 system using FACT /5/. All elements were assumed to be pure and in their standard state. The mole ratios of Mg and Zr with respect to (Al+Mg+Zr) were maintained at 0.1 at a temperature of 927 °C (1200K). The resultant Thermodynamic Stability Diagram is shown in Figure 14. The absence of Al_3Zr from any of the phase regions is particularly noteworthy. Increases in Zr mole fraction up to 0.3 did not result in any appreciable change in the stable species or their relative areas of stability. The experimental evidence of the formation of Al_3Zr can therefore be explained as follows.

When carrying the experiments under close to 1 atm N_2 pressure and with the absence of any detectable nitrides, the oxygen partial pressure may be smaller than 6×10^{-20} atm. Hence, under the experimental conditions of the static and the dynamic tests Al_2O_3, $MgAl_2O_4$ and ZrO_2 must be the stable phases at the alloy-substrate-gas interface. The formation of Al_3Zr must therefore be occurring purely from the direct contact between the alloy and the ZrO_2 substrate in the absence of a gas atmosphere.

It follows then that the sequence of events leading to metal-substrate reaction must be preceded by a complete breakdown of the alloy surface oxide. This breakdown occurs due to high temperature, alloying of aluminum with magnesium and the presence of a nitrogen atmosphere. The sample is held under these conditions for considerable time. As the liquid alloy is exposed to the atmosphere, there is constant destabilization of new surface oxide that forms on freshly exposed surface of the molten alloy. This process continues as the exposed alloy flows over the substrate until molten alloy contacts substrate in the absence of the gas atmosphere (i.e. the underside of the substrate). In our static experiments, this occurs in the region of the substrate adjacent to the graphite crucible leading to the extensive reactions shown in Figure 6.

This result illustrates the importance and difficulties in processing these Al based MMCs in a controlled manner. On the one hand the surface oxide impedes good melt-substrate or reinforcement contact. On the other hand, once good contact is achieved extensive reactions occur between the melt and the reinforcement. This can yield to undesirable and uncontrollable reaction products and degrade composite properties. The key to successful processing of these MMCs lies in the utilization of a partially degraded oxide to provide good bonding between melt and reinforcement. This may be achieved through the control of the time contact.

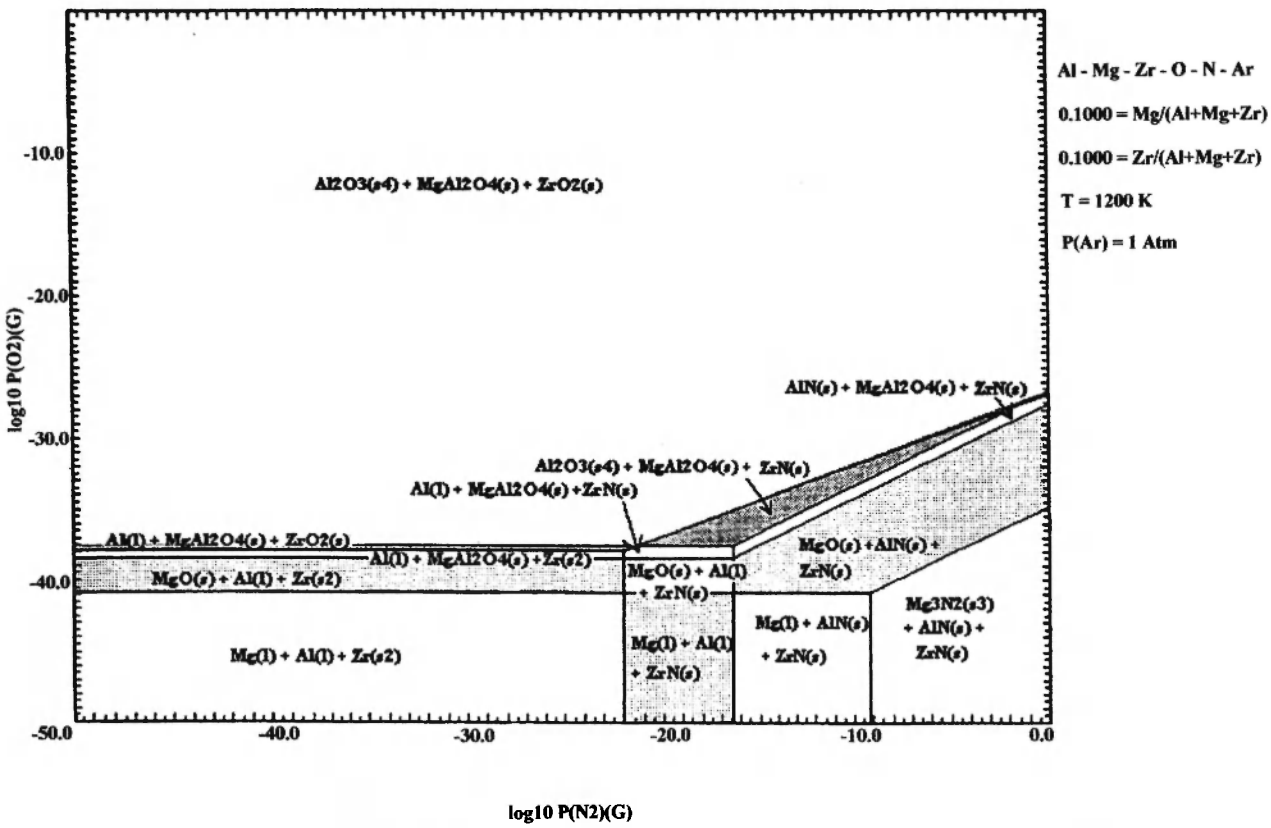

Fig. 14: Thermodynamic stability diagram for the Zr-Al-Mg-O-N system calculated using FACT.

Note that in the dynamic tests with Al-Mg alloy, at high temperature and under nitrogen gas, no metal flow was observed.

SUMMARY

Static and dynamic deposition experiments were carried out using Al and Al-10Mg on Al_2O_3 and ZrO_2 fully dense substrates. Different combinations of experimental conditions included varying metal and substrate temperatures from about 700 to 1000 °C, and using N_2 as the gas atmospheres with varying exposure times. Visual observations of the samples showed that in all cases there appeared to be good bonding between metal and substrate. However, for the sample carried out with Al-10Mg in a N_2 atmosphere at 1000 °C, the molten metal spread over the Al_2O_3 and ZrO_2 substrates and extensive reactions were observed at the interface on the underside of the ZrO_2 substrate after 3 hours of contact time.

From these observations and with the aid of FACT, an analysis of these experimental results revealed the following. Since magnesium is surface active and very reactive, the chemistry of the surface on the metal is modified to be closer to that of the spinel, which clearly lowers the melting point of the surface oxide. In addition, there is a favorable driving force for the extensive vaporization of magnesium into the atmosphere. Furthermore, Al_2O and Al gases have comparable vapor pressures and are likely to also vaporize from the surface oxide and the melt. The vaporization of Mg, Al_2O and Al will contribute to the destabilization of the surface oxide and a reduced interfacial tension between the melt and the substrate. The presence of N_2 as the gas atmosphere promotes the continuous vaporization of Al by the thermodynamically favored formation of AlN. All of these factors seem to work together to break down the tenacious oxide on the surface of aluminum and result in favorable wetting between melt and ceramic substrate. Finally, increasing temperature enhances the

thermodynamics of all of these mechanisms to the point where the alloy freely flows. Subsequent reaction between the alloy and the substrate in the absence of the gas atmosphere results in the formation of Al_3Zr intermetallic as one of the prominent reaction products.

Clearly, more research is needed to determine the kinetics of these reactions and to develop methodologies to control them in order to process an MMC with the desirable mechanical properties.

ACKNOWLEDGEMENTS

The assistance of Ms. Meenaxi Kahera of Westaim Corp and Ms. Tuyet Le, Mr. Louis Morin and Ms. Tina Barker of the Advanced Materials and Processing Lab, University of Alberta, in sample preparation and the conduct of the experiments and SEM analysis is acknowledged. In addition, the authors wish to thank the Metal Matrix Composites Consortium and the NSERC CR&D Program for their financial support.

REFERENCES

1. D. Huda, M. A. El Baradie, M. S. J. Hashmi, *Journal of Material Processing Technology*, **37**, 513-528 (1993).
2. J. C. Lee, K. N. Subramian, Y. Kim, *Journal of Material Science*, **29** (7-8), 1983-1990 (1994).
3. R. M. Cannon, B. J. Dalgleish, R.H. Dauskardt, T.S. Oh, R. O. Ritchie, *Acta Metallurgica et Materialia*, **39** (9), 2145-2156 (1991).
4. T. Suzuki, H. Umehara, R. Hayashi, *Journal of Material Science*, **8** (10), 2492-2498 (1993)..
5. *F*A*C*T 2.1 - User Manual'*, C. W. Bale, A. D. Pelton, W. T. Thompson, Ecole Polytechnique de Montreal / Royal Military College, Canada, July 1996. (http://www.crct.polymtl.ca).
6. L. Morin, M. Rieder, J. Meja and H. Henein, *Proceedings of the International Symposium on Light Metals 1996*, M. Avedesian, R. Guilbault and D. Ksinsik, Eds., Met. Soc. of CIM, Montreal, 1996, p. 293-304.
7. K. Olsen, G. Sterzik and H. Henein, *Third International Symposium: Recycling of Metals and Engineered Materials*, P.B. Queneau and R.D. Peterson, Eds, TMS, Warrendale, PA, 1995, p. 67-83.
8. T, Le and H. Henein: unpublished research, University of Alberta, Edmonton, AB, 1997.
9. G. Hass, *Optik*, **1** (8), 134-143 (1946).
10. G. Kaptay, *Materials Science Forum*, **77**, 315-330 (1991).
11. B.C. Pai, G. Ramani, R.M. Pillai and K.G. Satyanarayana, *Journal of Materials Science*, **30**, 190-3-1911 (1995).
12. Y. Le Petitcorps, J.M. Quenisset, G. Le Borgne and M. Barthole, *Materials and Engineering*, **A135**, 37-40 (1991).
13. J. L. Murray, *Bulletin of Alloy Phase Diagrams*, **3** (2), 60-74 (1982)..
14. P. Nicholson, McMaster University, private communications, October 7, 1997.
15. D.R. White, A.W. Urquhart, M.K. Aghajanian and D.K. Creber, US Patent 4,828,008, May 9, 1989.